

Dissociation Energies of Molecular Hydrogen and the Hydrogen Molecular Ion

Y. P. Zhang, C. H. Cheng,* J. T. Kim,† J. Stanojevic, and E. E. Eyler

Physics Department, University of Connecticut, Storrs, Connecticut 06269, USA

(Received 31 July 2003; published 20 May 2004)

We have obtained improved values for the dissociation energies of molecular hydrogen and its ion by using a high-resolution pulse-amplified laser to probe the second dissociation limit. The onset of the vibrational continuum is observed by state-selective detection of the atomic products of dissociation, and several auxiliary measurements link the results to the ground state. The dissociation energies are accurate to 0.010–0.026 cm^{-1} , improving previous measurements by a factor of 3–7. Agreement with *ab initio* calculations is good for H_2 , D_2 , and their ions, but not for HD and HD^+ .

DOI: 10.1103/PhysRevLett.92.203003

PACS numbers: 33.15.Fm, 33.80.Gj, 33.80.Rv

The hydrogen molecule and its ion are the simplest of all molecules, and thus play pivotal roles in molecular spectroscopy and quantum mechanics. The dissociation energies (D_0) of both species have long served as benchmarks for *ab initio* calculations [1,2], including accurate treatments of nonadiabatic, relativistic, and radiative effects. Recent experimental determinations have been based primarily on measurements of the second dissociation limit, $\text{H}(1s) + \text{H}(2s \text{ or } 2p)$, because this is the lowest atomic asymptote for which the dissociation continuum has so far been observed. The best of these experiments attained accuracies of about 0.04 cm^{-1} , an improvement by an order of magnitude compared with the first high-resolution study by Herzberg [3,4]. The group of Stoicheff used fluorescence spectroscopy near 84.5 nm to measure the onset of dissociation at the second dissociation limit for all three stable isotopes, H_2 , D_2 , and HD [5]. The second dissociation limit has also been studied by our own research group using laser double resonance through the double-minimum EF state [6,7].

A few years ago, our group showed that spectra can be obtained near the second dissociation limit with much higher resolution, up to 0.003 cm^{-1} , by selectively detecting the atomic products of dissociation [8]. Here we report new measurements of D_0 obtained with this detection method, using the overall scheme shown in Fig. 1. We perform two-step excitation through vibrational levels of the EF state having energies close to the top of the barrier of the double-well potential, $v = 6$ for H_2 and HD, and $v = 9$ for D_2 . These levels have vibrational amplitudes spanning a wide range of internuclear separations, giving favorable Franck-Condon overlaps both with the ground state and with the near-threshold continuum region.

This determination of D_0 is the culmination of a multi-year effort that involves three separate sets of experimental measurements. First, we determined the term energies of several rotational levels of the $EF \ ^1\Sigma_g^+$ state with $v = 0$, to an accuracy of about 0.0008 cm^{-1} , or 7 parts in 10^9 . This measurement, accomplished by means of Doppler-free two-photon excitation at 202 nm using a carefully characterized pulse-amplified laser system, is

described in Ref. [9]. Unfortunately, vibrationally excited levels of the EF state cannot be measured by the same method, because the required wavelengths cannot readily be produced by frequency tripling.

Our second set of measurements sidesteps this limitation by using an indirect method to determine the energies of vibrationally excited EF state levels, v^* , relative to $v = 0$. This is accomplished by measuring transitions both from $EF, v = 0$ and from EF, v^* to a common low- n Rydberg state, then taking appropriate differences. These experiments, as well as numerous accurate Rydberg state term energies that resulted from them, are described in a forthcoming publication [10]. A representative example is the $v = 6, N'' = 1$ level of H_2 , which is calibrated using three measurements: (1) $EF \leftarrow X, (0-0)$ band, $Q(1)$ branch at 99 109.7320(7) cm^{-1} , (2) $D \ ^1\Pi_u^- \leftarrow EF, (2-0)$, $Q(1)$ at 18 019.6476(8) cm^{-1} , and (3) $D \ ^1\Pi_u^- \leftarrow EF, (2-6)$, $Q(1)$ at 13 642.2565(16) cm^{-1} .

The third and final portion of the experimental program is the analysis of the near-threshold continuum

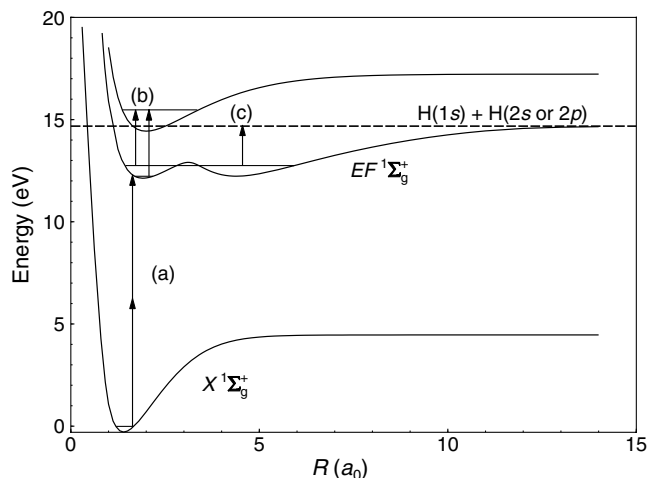


FIG. 1. Overall scheme for measuring D_0 . Three separate experiments are involved: (a) Measure $EF, v = 0$; (b) Measure $EF, v = 6$ ($v = 9$ for D_2) relative to $v = 0$; (c) Determine the second dissociation limit by exciting it from $EF, v = 6$.

excited from EF , $\nu = 6$ or $\nu = 9$, and the determination of D_0 from the results. In total, we have measured 11 such thresholds as indicated in Table I, including at least two for each isotopic variant. In the interest of brevity, we select two examples for detailed discussion in this Letter. One, the $2s + 2p$ threshold of H_2 excited from $N'' = 1$, is a special case for which an exceptionally accurate determination of the threshold proved possible. The other, the $H(1s) + D(2s)$ threshold of HD with $N'' = 0$, is a fairly representative sample of the remaining threshold spectra. A fuller account of the others is provided in Ref. [10].

The experimental setup is similar to that of Ref. [8]. A 193 nm broadband pump laser populates the $EF \ ^1\Sigma_g^+$ ($\nu = 6$) state, then a high-resolution 677 nm pulse-amplified laser probes the region of the second dissociation limit. This laser, with a bandwidth of about 90 MHz, intersects at right angles a collimated supersonic beam of molecular hydrogen. We use a pentaprism to set the intersection angle within 3 mrad, limiting the Doppler shift to ≤ 10 MHz. Optical phase perturbations in the pulsed amplifier are measured by optical heterodyne beat methods [11]. Excited hydrogen atoms produced by predissociation are detected with an auxiliary detection laser that excites $2s$ and $2p$ atoms to $n = 40$ Rydberg states, which are efficiently detected by pulsed field ionization. By firing the photodissociation and detection lasers simultaneously, we can detect dissociation from both the $2s$ and $2p$ atomic states, as well as some of the highest bound molecular levels just below threshold. If we delay the detection laser pulse, only metastable $2s$ atoms are detected. We obtain both absolute frequency calibrations and reproducible frequency markers from the hyperfine spectrum of iodine, using a saturation spectrometer and the iodine atlas from Toptica Photonics AG. To reduce the effects of slow intensity fluctuations, we typically average the results of three independent scans, after aligning the

spectral data within 1.5 MHz by using a correlation analysis of selected iodine reference lines.

Measurements have been performed for initial rotational levels $N'' = 0$ and $N'' = 1$ in H_2 , D_2 , and HD . To determine the dissociation limit, we rely on analysis of the near-threshold vibrational continuum because the highest bound levels have not been calculated with sufficient accuracy to permit accurate extrapolation. Unfortunately, the continuum often exhibits multiple thresholds and complicated structure caused by nonadiabatic electronic couplings, spin interactions, and shape resonances. For the moment we ignore these effects, which will be considered below. In this simplified case only transitions to the $B' \ ^1\Sigma_u^+$ state have appreciable amplitudes, because the $B \ ^1\Sigma_u^+$ state has extremely small Franck-Condon factors and the $C \ ^1\Sigma_u^+$ potential has a barrier about 100 cm^{-1} high that prevents direct dissociation [12]. The B' potential converges to $H(1s) + H(2s)$, so no $2p$ atoms would be observed in the adiabatic approximation.

Very close to threshold, the continuum cross section σ should follow the Wigner threshold law, $\sigma \propto E^{N+1/2}$. Thus, photodissociation from EF , $N'' = 0$, for which only the R branch is allowed, should exhibit a $E^{3/2}$ power law. From the $N'' = 1$ rotational level, continua with both $N = 0$ and $N = 2$ are accessible, but the centrifugal barrier for $N = 2$ suppresses this channel in the immediate threshold vicinity. Numerical calculations for a spinless adiabatic H_2 molecule confirm that photodissociation from $N'' = 1$ accurately follows the Wigner law for an $N = 0$ continuum, at least for the first 0.1 cm^{-1} or so above threshold [12]. Our data analysis relies primarily on Wigner law fits extending over this range, although in nearly all cases it is necessary to consider the effects of complications due to nonadiabatic coupling or atomic fine structure (fs) and hyperfine structure (hfs).

A drastic departure from adiabatic behavior occurs for the first example that we consider in detail, the $N'' = 1$ threshold for H_2 , shown in Fig. 2. In this special case a strong atomic $2p$ signal is observed with a very rapid continuum onset, probably associated with the broad R^{-3} potential of the B state, that facilitates accurate threshold determination. Nonadiabatic mixing of the B , B' , and C states is enhanced by the presence of a strong shape resonance to the C state only about 0.2 cm^{-1} above threshold [8]. Unfortunately, this same nonadiabatic mixing leads also to a strong bound-state spectrum that includes high- ν levels of the B state and probably also its triplet counterpart. The continuum onset is overlapped by the highest observed bound level, which in turn is not fully resolved from the second-highest level, near 0.138 cm^{-1} in Fig. 2. Even though we have evidence that both of these levels are stable [10], they might conceivably be quasibound resonances lying above the lowest atomic threshold, $H(1s, F = 0) + H(2p_{1/2})$. Indeed, analogous long-lived resonances have very recently been reported at the $5s + 5p$ threshold of Rb_2

TABLE I. Dissociation limits from the EF state and corresponding D_0 values, both in cm^{-1} , relative to the center of gravity (COG) of the $1s_{1/2}$ hyperfine structure. Measurements are from $\nu = 6$ for H_2 and HD , and from $\nu = 9$ for D_2 .

	N''	Threshold	Dissoc. limit	D_0
H_2	0	$1s + 2s$	14 817.414(23) ^a	36 118.054(23)
	0	$1s + 2s$	14 817.413(25) ^b	36 118.053(25)
	1	$1s + 2p_{1/2}$	14 771.375(12) ^a	36 118.065(12)
	1	$1s + 2s$	14 771.405(23)	36 118.060(23)
D_2	0	$1s + 2s$	14 833.049(15)	36 748.346(15)
	1	$1s + 2s$	14 807.169(12)	36 748.340(12)
HD	0	$D(1s) + H(2s)$	15 443.963(21)	36 405.822(21)
	1	$D(1s) + H(2s)$	15 402.872(16)	36 405.829(43)
	0	$H(1s) + D(2s)$	15 466.366(17) ^a	36 405.843(18)
	0	$H(1s) + D(2s)$	15 466.363(20) ^b	36 405.840(21)
	1	$H(1s) + D(2s)$	15 425.222(25)	36 405.797(47)

^aMeasured for $F = 0$ and referred to the COG.

^bMeasured for $F = 1$ and referred to the COG.

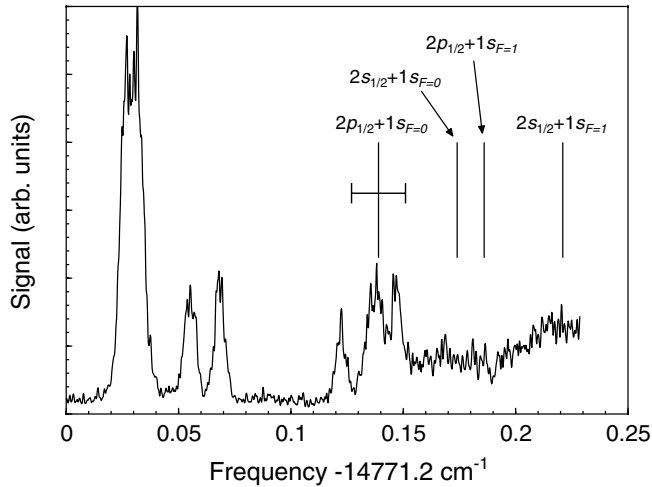


FIG. 2. Highest bound states and adjoining vibrational continuum at the second dissociation limit of H_2 , excited from the $\nu = 6$, $N'' = 1$ level of the E, F state. Atomic fs and hfs thresholds are indicated by vertical lines and error bar, corresponding to the results given in Table I.

[13]. Therefore, we set a conservative lower bound for the $F = 0$ threshold below the second-highest bound level, where there is no observable continuum signal in our lowest-power spectra. We set an upper bound above the highest bound level by adding its linewidth to its center frequency. In Table I we use the average of these two bounds, with an uncertainty of half their difference.

Our other example, the HD threshold shown in Fig. 3, is more representative of what is typically observed. Here no $D(2p)$ atoms are observed, and the continuum onset is more gradual, extending over an energy scale matching our predictions for the B' state continuum. In addition to the initial threshold onset, a second threshold corresponding to the $\text{H}(1s, F = 1)$ hyperfine level is observable as a discontinuity of the continuum slope, so we fit the data to a sum of two Wigner threshold laws. The difference between the two thresholds obtained from the fit agrees

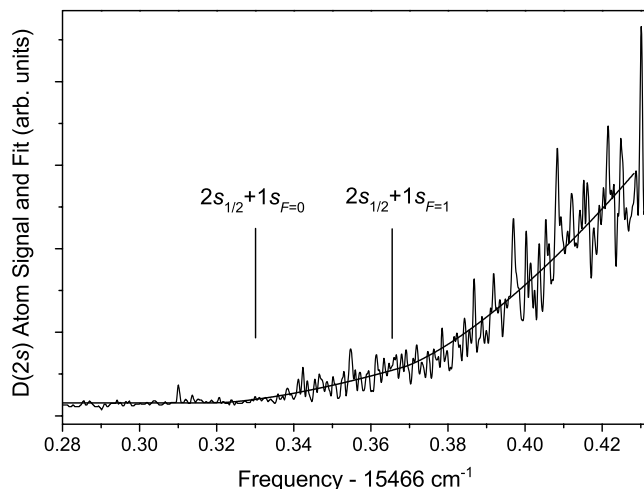


FIG. 3. Dissociation of HD, $N'' = 0$, to $\text{H}(1s) + \text{D}(2s)$.

with the known hyperfine splitting within 90 MHz. It is worth noting that in one regard, this threshold is not entirely well behaved. It is the same one for which we have previously reported an unusual threshold-related resonance in the continuum of the other energetically allowed product channel, $\text{D}(1s) + \text{H}(2s)$ [8]. However, this seems to have no obvious effect on the shape of the continuum offset in the $\text{D}(2p)$ channel shown here.

Because many of the thresholds show obvious deviations from the Wigner law, a careful analysis of the model-dependent uncertainty is required, and this is generally the largest contribution to the error budget. First, we conservatively estimate the dependence on the ending point of the Wigner law fit by taking the difference δ_1 between fits with the smallest reasonable ending point and the largest reasonable ending point. We similarly estimate the dependence δ_2 on the starting point, which is sensitive primarily to fluctuating background levels or contamination of the spectrum by bound states. Finally, we estimate the dependence on the form of the power law, by taking the difference δ_3 between fits to a fixed power law and a variable power law. Our estimate of the total model-dependent uncertainty is the quadrature sum of all three contributions. For the HD example of Fig. 3, $\delta_1 \approx 378$ MHz, $\delta_2 \approx 108$ MHz, and $\delta_3 \approx 216$ MHz.

In some cases, the ground-state hyperfine doublet is not resolved due to noise or, in the case of the D atom, due to its small size, producing another significant uncertainty. The spectrum just above the observed dissociation limit corresponds purely to the lower hfs limit, whereas the spectrum well above threshold should converge to the center of gravity (COG) of the hfs levels. Thus, it seems safe to say that the result lies between the lower hfs level, a lower bound, and the COG, an upper bound. As before, we use the average of these bounds, with an uncertainty of half their difference.

Table II shows the error budget for the HD example, including the above contributions and several smaller effects, such as the unresolvably small $n = 2$ hfs [14]. In some cases the ac Stark shift of the threshold could not be measured directly, so we estimated its uncertainty by using the worst case of the measurable shifts, evaluated for the average irradiance used in each set of measurements. The total uncertainty is taken to be the quadrature sum of several independent contributions.

TABLE II. Error budget in cm^{-1} of D_0 for the example of HD, $N'' = 0$, $\text{H}(1s) + \text{D}(2s)$.

Model dependence and hfs correction	0.0150
ac Stark shift	0.0130
EF , $\nu = 6$ term energy (Refs. [9,10])	0.0055
Weighted statistical uncertainty	0.0030
I_2 atlas calibration	0.0020
All other uncertainties (quadrature sum)	0.0010
Total	0.021

TABLE III. Recent experimental measurements and *ab initio* calculations of D_0 and D_0^+ in cm^{-1} . “Offset” values should be added to all rows except Δ , which denotes differences between this work and theory from Refs. [1,16].

	H_2	D_2	HD
Offset	36 118	36 748	36 405
Expt. [3,4]	0.6(5)	0.9(4)	1.2(4)
Expt. [5]	0.11(8)	0.38(7)	0.83(10)
Expt. [7]	0.06(4)	0.32(7)	0.88(10)
This work	0.062(10) ^a	0.343(10)	0.828(16)
Theory [2]	0.049	0.345	0.763
Theory [1]	0.069	0.364	0.787
Δ	-0.007	-0.021	0.041

	H_2^+	D_2^+	HD^+
Offset	21 379	21 711	21 516
Expt. [5]	0.37(8)	0.64(7)	0.12(10)
This work	0.343(14)	0.595(26)	0.112(20)
Theory [16]	0.350	0.583	0.070
Δ	-0.007	0.012	0.042

^aIf we assume the highest observed level in Fig. 2 is below the $F=0$ threshold, the result becomes $D_0(\text{H}_2) = 36\,118.073(4) \text{ cm}^{-1}$.

Our results for the threshold energies are summarized in Table I. The largest uncertainties are generally those due to model dependence, unresolved hfs, and the ac Stark shift. Each of the results is determined by a statistical weighted average of different runs. In finding the weights, we exclude the systematic uncertainties that are common to all runs. They are later added in quadrature to find the total uncertainty.

To obtain the ground-state dissociation energy D_0 , we add our measured values for the EF state term energies [9,10], and subtract the atomic $1s$ - $2s$ intervals [15]. The last column in Table I tabulates the results. For all three isotopic variants, there are multiple determinations, and their consistency is well within the combined uncertainties. The weighted averages of D_0 are shown in Table III. Our results are about 4–7 times more accurate than the best previous measurements. Agreement with the latest theoretical D_0 values [1], thought to be accurate to $\leq 0.02 \text{ cm}^{-1}$, is good for H_2 and D_2 , but poor for HD.

We can also determine improved dissociation energies D_0^+ for the molecular ion, by combining our results with the atomic ionization potential (IP) [17] and the molecular IP, for which we use recent experimental determinations [18–22]. In the case of H_2 we use a weighted average of Refs. [18–20] to obtain an IP of $124\,417.491(10) \text{ cm}^{-1}$. The results for D_0^+ are shown in the lower part of Table III, together with other recent experimental evaluations and *ab initio* calculations. These results again agree with recent theoretical calculations [16] for H_2^+ and D_2^+ , but not for HD^+ . The discrepancy for HD^+ is noteworthy,

because the theoretical accuracy is thought to be as good as 0.01 cm^{-1} . We can think of no likely experimental explanation, unless there is an unpredicted long-range potential barrier in HD.

The present experimental accuracy now exceeds that of theory for D_0 , although not for D_0^+ . A new measurement of the molecular IP, now underway in our laboratory, should further improve the accuracy of D_0^+ . We hope that these results will stimulate further theoretical work on both of these fundamental systems.

We thank Hyewon Kim for valuable assistance.

*Present address: Panasonic Boston Laboratory, 68 Rogers Street, Cambridge, MA 02142, USA.

†Present address: Department of Photonic Engineering, Chosun University, Gwangju, 501-759 Korea.

- [1] L. Wolniewicz, *J. Chem. Phys.* **103**, 1792 (1995).
- [2] W. Kolos and J. Rychlewski, *J. Chem. Phys.* **98**, 3960 (1993).
- [3] G. Herzberg, *J. Mol. Spectrosc.* **33**, 147 (1970).
- [4] W. C. Stwalley, *Chem. Phys. Lett.* **6**, 241 (1970).
- [5] A. Balakrishnan, V. Smith, and B. P. Stoicheff, *Phys. Rev. Lett.* **68**, 2149 (1992); *Phys. Rev. A* **49**, 2460 (1994); A. Balakrishnan, M. Vallet, and B. P. Stoicheff, *J. Mol. Spectrosc.* **162**, 168 (1993).
- [6] E. F. McCormack and E. E. Eyler, *Phys. Rev. Lett.* **66**, 1042 (1991).
- [7] E. E. Eyler and N. Melikechi, *Phys. Rev. A* **48**, R18 (1993).
- [8] C. H. Cheng, J. T. Kim, E. E. Eyler, and N. Melikechi, *Phys. Rev. A* **57**, 949 (1998).
- [9] A. Yiannopoulou, N. Melikechi, S. Gangopadhyay, J. C. Meiners, and E. E. Eyler (to be published).
- [10] Y. P. Zhang, C. H. Cheng, H. Kim, J. T. Kim, J. Stanojevic, and E. E. Eyler (to be published).
- [11] S. Bergeson *et al.*, *Phys. Scr.* **T83**, 76 (1999).
- [12] C. W. Zucker and E. E. Eyler, *J. Chem. Phys.* **85**, 7180 (1986).
- [13] M. Kemmann *et al.*, *Phys. Rev. A* **69**, 022715 (2004).
- [14] S. R. Lundeen, P. E. Jessop, and F. M. Pipkin, *Phys. Rev. Lett.* **34**, 377 (1975).
- [15] Th. Udem *et al.*, *Phys. Rev. Lett.* **79**, 2646 (1997); A. Huber *et al.*, *Phys. Rev. Lett.* **80**, 468 (1998).
- [16] C. A. Leach and R. E. Moss, *Annu. Rev. Phys. Chem.* **46**, 55 (1995).
- [17] G. W. Erickson, *J. Phys. Chem. Ref. Data* **6**, 831 (1977).
- [18] E. McCormack, J. M. Gilligan, C. Cornaggia, and E. E. Eyler, *Phys. Rev. A* **39**, 2260 (1989).
- [19] C. Jungen, I. Dabrowski, G. Herzberg, and M. Vervloet, *J. Chem. Phys.* **93**, 2289 (1990).
- [20] A. de Lange, E. Reinhold, and W. Ubachs, *Phys. Rev. A* **65**, 064501 (2002).
- [21] C. Jungen, I. Dabrowski, G. Herzberg, and M. Vervloet, *J. Mol. Spectrosc.* **153**, 11 (1992).
- [22] J. M. Gilligan and E. E. Eyler, *Phys. Rev. A* **46**, 3676 (1992).